Theoretical Studies of Organometallic Compounds. 4.[1] Chelate Complexes of $TiCl_4$ and CH_3TiCl_3

Volker Jonas and Gernot Frenking*

Fachbereich Chemie, Universität Marburg, Hans-Meerwein-Strasse, D-3550 Marburg, Germany

Manfred T. Reetz

Max-Planck-Institut für Kohlenforschung, Kaiser-Wilhelm-Platz 1, D-4330 Mülheim an der Ruhr 1, Germany

Received December 23, 1992

The equilibrium structures and binding energies of chelate complexes of $TiCl_4$ and CH_3TiCl_3 with various bidentate ligands have been studied theoretically using effective core potentials and model potentials at the Hartree–Fock and MP2 levels of theory. The results are compared with experiments.

Introduction

In the first paper of this series[2] we reported the results of a systematic investigation using effective core potentials (ECP) and model potentials (MP) for predicting geometries and energies of isodesmic reactions of the tetrahedral transition-metal compounds $Ti(CH_3)_nCl_{4-n}$ (n = 0–4). We studied the effect of splitting the valence shell basis set and the performance of several ECP methods with different core sizes and compared them to results obtained from all electron basis sets. The best overall agreement with experimental geometries and energies is obtained when the $(n-1)s^2$ $(n-1)p^6$ $(n-1)d^a$ ns^b ECP developed by Hay and Wadt[3] with the contraction scheme (441/2111/41) is used.[2]

We now turn to chemically more interesting compounds. $TiCl_4$ may form octahedral complexes with various ligands L as either the monomer $TiCl_4L_2$ or dimer $(TiCl_4L)_2$. With bidentate ligands Bid, $TiCl_4$ forms chelate complexes $TiCl_4Bid$. CH_3TiCl_3 is also known to form octahedral complexes. Chelate complexes are important compounds in stereoselective reactions because the formation of chelates as intermediates may strongly influence the stereoselectivity of nucleophilic addition reactions.[4] Unfortunately, little experimental data are available concerning the structure and stability of chelate complexes.[5-13]

In order to gain more information about this important class of molecules, we investigated theoretically the structures and binding energies of the octahedral complexes of the Lewis acids $TiCl_4$ (1) and CH_3TiCl_3 (2) with the bidentate chelating ligands 3–11 shown in Figure 1. The calculated chelate complexes 12–26 are shown in Figure 2.

X-ray structure analyses have been published for two of the investigated complexes, i.e., molecules 13 and 16.[5,6] There are no experimental results available for the other calculated complexes. However, related compounds have been studied experimentally and may be used for comparison. The results of a neutron diffraction investigation and an X-ray structure analysis of the CH_3TiCl_3 complex with $Me_2PCH_2CH_2PMe_2$ shows that the methyl group at Ti occupies an equatorial position trans to the PMe_2 group.[13] NMR studies of complexes of 2 with several symmetrical[14] and unsymmetrical[15] ligands XCH_2CH_2Y (X, Y = OMe, SMe, NMe_2) also indicate that the methyl group at titanium occupies an equatorial rather than an axial position. Furthermore, the methyl group at Ti is found to be trans to the harder[16] donor group. For example, in the complex of $Me_2NCH_2CH_2OMe$ with 2 the methyl group at Ti is trans to OMe.[15]

Chelate complexes of $TiCl_4$ and CH_3TiCl_3 have been utilized as versatile agents for stereoselective organic synthesis.[4,17] For example, CH_3TiCl_3 reacts with chiral α-alkoxy carbonyl compounds 27 (Scheme I) with high diastereoselectivity to form chelation-controlled adducts. Octahedral chelate complexes 28 as intermediates have been suggested to account for the observed diastereoselectivity, which is opposite to what is predicted by the Felkin–Anh model.[18]

Later, these Cram-type chelates were observed directly by ^1H and ^{13}C NMR spectroscopy.[19] Since the ligands are not symmetrical, four diastereomeric octahedral chelates

(1) Part 3: Veldkamp, A.; Frenking, G. *J. Comput. Chem.* **1992**, *13*, 1184.
(2) Jonas, V.; Frenking, G.; Reetz, M. T. *J. Comput. Chem.* **1992**, *13*, 919.
(3) Hay, P. J.; Wadt, W. R. *J. Chem. Phys.* **1985**, *82*, 299. The ECP's for the transition metals with a $(n-1)$s $(n-1)$p $(n-1)$d ns valence space is described as the third paper of a series and therefore termed HW3.
(4) Reetz, M. T. *Angew. Chem.* **1984**, *96*, 542; *Angew. Chem., Int. Ed. Engl.* **1984**, *23*, 556.
(5) Viard, B.; Poulain, M.; Grandjean, D.; Amaudrut, J. *J. Chem. Res., Synop.* **1983**, *84*, 853.
(6) Maier, G.; Seipp, U.; Boese, K. *Tetrahedron Lett.* **1987**, *28*, 4515.
(7) Poll, T.; Metter, J. O.; Helmchen, G. *Angew. Chem.* **1985**, *97*, 116; *Angew. Chem., Int. Ed. Engl.* **1985**, *24*, 112.
(8) Utko, J.; Sobota, P.; Lis, T. *J. Organomet. Chem.* **1987**, *334*, 341.
(9) Utko, J.; Sobota, P.; Lis, T. *J. Organomet. Chem.* **1989**, *373*, 63.
(10) Sobota, P.; Utko, J.; Lis, T. *J. Organomet. Chem.* **1990**, *393*, 349.
(11) Oppolzer, W.; Rodriguez, I.; Blagg, J.; Bernardinelli, C. *Helv. Chim. Acta* **1989**, *72*, 123.
(12) Bott, S. G.; Prinz, H.; Alvanipour, A.; Atwood, J. L. *J. Coord. Chem.* **1987**, *16*, 303.
(13) Dawoodi, Z.; Green, M. L. H.; Mtetwa, V. S. B.; Prout, K.; Schultz, A. J.; Williams, J. M.; Koetzle, T. F. *J. Chem. Soc., Dalton Trans.* **1986**, 1629.
(14) Clark, R. J. H.; McAlees, A. J. *J. Chem. Soc. A* **1970**, 2026.
(15) Clark, R. J. H.; McAlees, A. J. *Inorg. Chem.* **1972**, *11*, 342.
(16) (a) Pearson, R. G. *J. Am. Chem. Soc.* **1963**, *85*, 3533. (b) Pearson, R. G.; Songstad, J. *J. Am. Chem. Soc.* **1967**, *89*, 1827.
(17) Reetz, M. T. *Organotitanium Reagents in Organic Synthesis*; Springer: Berlin, 1986.
(18) (a) Chérest, M.; Felkin, H.; Prudent, N. *Tetrahedron Lett.* **1968**, 2201, 2205. (b) Anh, N. T.; Eisenstein, O. *Nouv. J. Chim.* **1977**, *1*, 61. (c) Anh, N. T. *Top. Curr. Chem.* **1980**, *68*, 145.
(19) Reetz, M. T.; Hüllmann, M.; Seitz, T. *Angew. Chem.* **1987**, *99*, 478; *Angew. Chem., Int. Ed. Engl.* **1987**, *26*, 477.

0276-7333/93/2312-2111$04.00/0

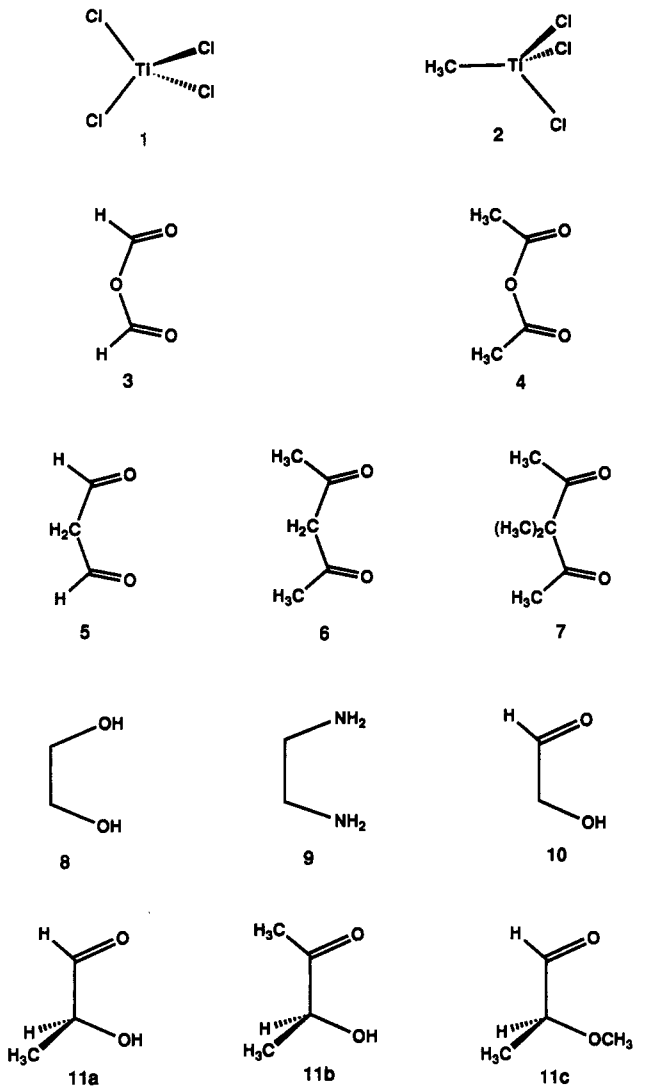

Figure 1. Donor and acceptor molecules treated in this study.

are possible, but only two are observed. It was proposed that the two complexes have methyl groups trans to the chelating donor ligand.

A more universal reaction scheme for chelation-controlled additions was also developed. In these reactions, α- and β-alkoxy aldehydes are treated with Lewis acids such as $TiCl_4$ and $SnCl_4$ to form an intermediate chelate which then reacts with suitable C-nucleophiles (Scheme II).[4,20] A recent rapid-injection NMR study[21] has revealed interesting results, which have been used by the authors to suggest what intermediates may be found during the reaction. We will compare our theoretical data with the experimental information.[21]

A question which is not addressed in the present investigation concerns the importance of "agostic" interactions.[22] In a recent study of the structure of the chelate complex of $H_2PCH_2CH_2PH_2$ with CH_3TiCl_3 it was shown[23] that the tilting angle of the methyl group and the decrease in the Ti–C–H bond angle can only be reproduced when correlation energy is included, e.g. at the MP2 level. It was also found[23] that the Ti–CH_3 bond distance is calculated too short by 0.04–0.07 Å at the Hartree–Fock level. Because the present theoretical study is concerned mainly with the structures and energies of the chelate complexes rather than agostic interactions, the conclusions drawn in this paper are not affected. The question of agostic interactions in the complexes investigated here will be the subject of a future study.[24]

Theoretical Methods

The calculations were performed using the program packages GAUSSIAN90,[25] TURBOMOL,[26] and CADPAC.[27] The geometries of the calculated molecules were optimized at the Hartree–Fock (HF) level of theory using two basis sets. For the calculations with the pseudopotential of Hay and Wadt[3] the contraction scheme (441/2111/41) at Ti has been employed.[2] The d functions consist of a set of five spherical functions each. The calculations with the spd model potential of Sakai and Huzinaga[28] were carried out with the contraction scheme (51/31/41).[2] In this case, the d functions consist of a set of six Cartesian functions. In both cases a 3-21G* basis set was used for the ligands which implies 3-21G(d)[29a] at Cl and 3-21G[29b] at C, N, O, and H. The resulting basis set combinations are shown in Table I.

Except for **15** and **16** all structures calculated with the Huzinaga model potential basis set I were verified as minima on the potential energy hypersurface by calculating the Hessian matrix analytically. Force constants have not been calculated with the Hay and Wadt ECP basis set II because analytical second derivatives are not available in the used program packages. Structures **15** and **16** have been verified as minima by optimizing the molecule with an all-electron basis set, calculating the Hessian matrix analytically, and then starting the optimization with basis set II. Structures **25a,b** and **26a,b** have been verified as minima by calculating the Hessian matrix numerically. The eigenvalues of the Hessian matrix are positive in all cases, which indicates that the structures are minima on the potential energy hypersurface at the respective level of theory.

Improved total energies have been calculated using the less contracted ECP[3] valence basis set (3311/2111/311) for Ti and the 6-31G(d)[30] basis set for the other atoms. This basis set is denoted basis set III. The d functions consist of a set of five spherical functions each. Correlation energy was calculated using Møller–Plesset perturbation theory[31] terminated at second order (MP2).

Unless otherwise noted, the geometries calculated with basis set II are used for the discussion because it has been shown that they are more reliable than those calculated with basis set I.[2] Relative energies are discussed using MP2/III values at HF/II

(20) Reetz, M. T.; Kesseler, K.; Schmidtberger, S.; Wenderoth, B.; Steinbach, R. *Angew. Chem.* **1983**, *95*, 1007; *Angew. Chem., Int. Ed. Engl.* **1983**, *22*, 989; *Angew. Chem., Suppl.* **1983**, 1511.

(21) Reetz, M. T.; Raguse, B.; Marth, C. F.; Hügel, H. M.; Bach, T.; Fox, D. N. A. *Tetrahedron* **1992**, *48*, 5731.

(22) Brookhart, M.; Green, M. L. H. *J. Organomet. Chem.* **1983**, *250*, 395.

(23) Weiss, H.; Haase, F.; Ahlrichs, R. *Chem. Phys. Lett.* **1992**, *194*, 492.

(24) Jonas, V.; Frenking, G.; Reetz, M. T., work in progress.

(25) Frisch, M. J.; Head-Gordon, M.; Trucks, G. W.; Foresman, J. B.; Schlegel, H. B.; Raghavachari, K.; Robb, M.; Binkley, J. S.; Gonzalez, C.; Defrees, D. J.; Fox, D. J.; Whiteside, R. A.; Seeger, R.; Melius, C. F.; Baker, J.; Martin, R. L.; Kahn, L. R.; Stewart, J. J. P.; Topiol, S.; Pople, J. A. Gaussian 90, Revision J; Gaussian: Pittsburgh, PA, 1990. We used the Convex, Silicon Graphics, Cray, and Fujitsu versions of the program package.

(26) Amos, R. D.; Rice, J. E. CADPAC: The Cambridge Analytical Derivatives Package, issue 4.0; Cambridge U.K., 1987. We also used issue 4.2 installed on the Cray Y-MP computer in Jülich.

(27) (a) Häser, M.; Ahlrichs, R. *J. Comput. Chem.* **1989**, *10*, 104. (b) Ahlrichs, R.; Bär, M.; Häser, M.; Horn, H.; Kölmel, C. M. *Chem. Phys. Lett.* **1989**, *162*, 165.

(28) Sakai, Y.; Miyoshi, E.; Klobukowski, M.; Huzinaga, S. *J. Comput. Chem.* **1987**, *8*, 256.

(29) (a) Gordon, M. S.; Binkley, J. S.; Pople, J. A.; Pietro, W. J.; Hehre, W. J. *J. Am. Chem. Soc.* **1982**, *104*, 2797. (b) Binkley, J. S.; Pople, J. A.; Hehre, W. J. *J. Am. Chem. Soc.* **1980**, *102*, 939.

(30) (a) Ditchfield, R.; Hehre, W. J.; Pople, J. A. *J. Chem. Phys.* **1971**, *54*, 724. (b) Hehre, W. J.; Ditchfield, R.; Pople, J. A. *J. Chem. Phys.* **1972**, *56*, 2257. (c) Francl, M. M.; Pietro, W. J.; Hehre, W. J.; Binkley, J. S.; Gordon, M. S.; DeFrees, D. J.; Pople, J. A. *J. Chem. Phys.* **1982**, *77*, 3654.

(31) (a) Møller, C.; Plesset, M. S. *Phys. Rev.* **1934**, *46*, 618. (b) Binkley, J. S.; Pople, J. A. *Int. J. Quantum Chem.* **1975**, *9*, 229.

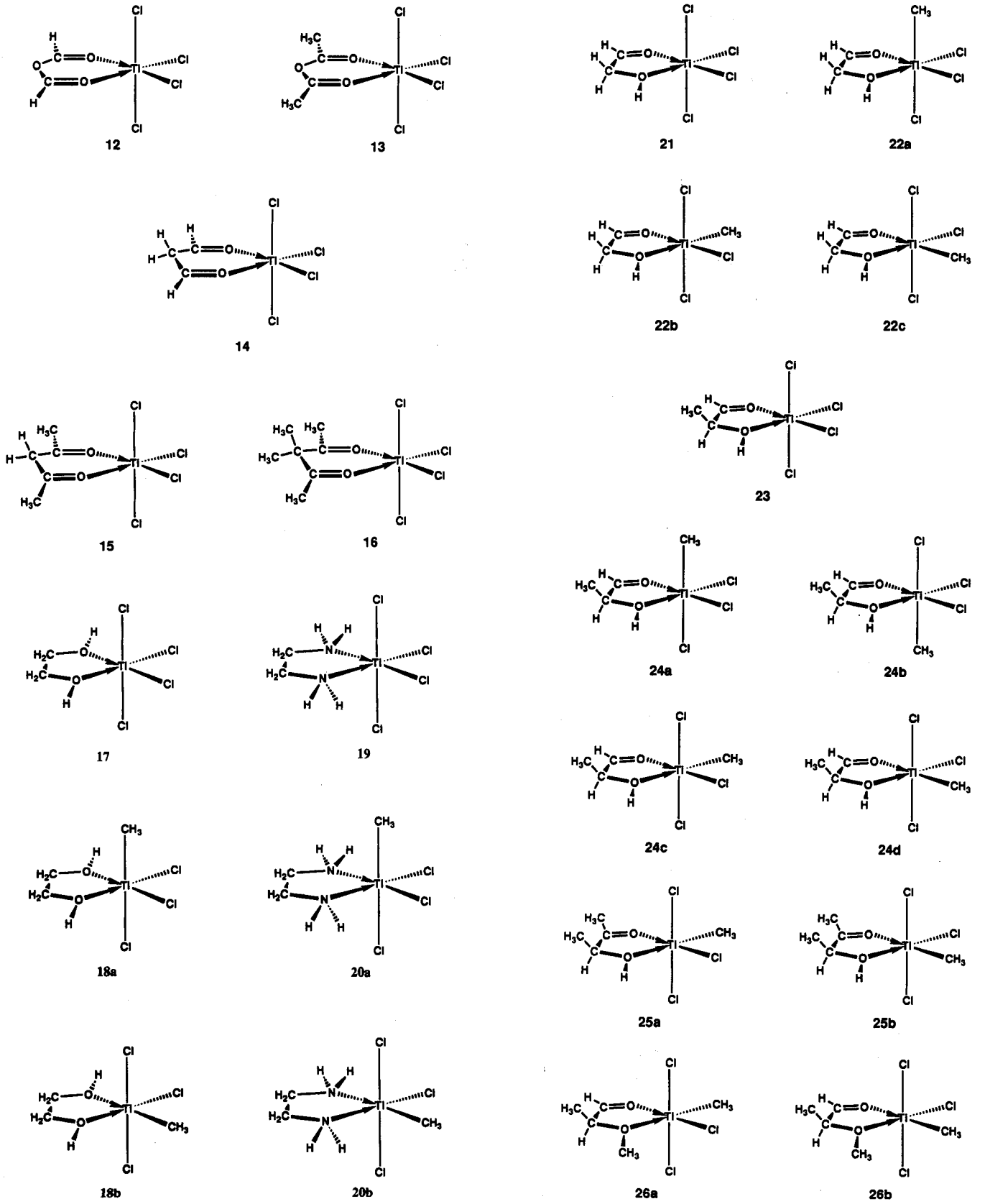

Figure 2. Calculated $TiCl_4$ and CH_3TiCl_3 complexes **12–26.**

optimized geometries. We will focus on the geometries of the complexes and the relative binding energies of the different donor ligands.

Results and Discussion

$TiCl_4$ Complexes of Formic and Acetic Acid Anhydrides (12, 13). The theoretically predicted energy minimum structures **12** and **13** and the experimental structure of **13** are shown in Figure 3. The calculated bond lengths and angles are shown in Table II together with the experimental data for **13**.

The complexes **12** and **13** are theoretically predicted to have C_{2v} symmetry (Figure 3); i.e., the six-membered ring is calculated as planar. The X-ray structure analysis of

Scheme I

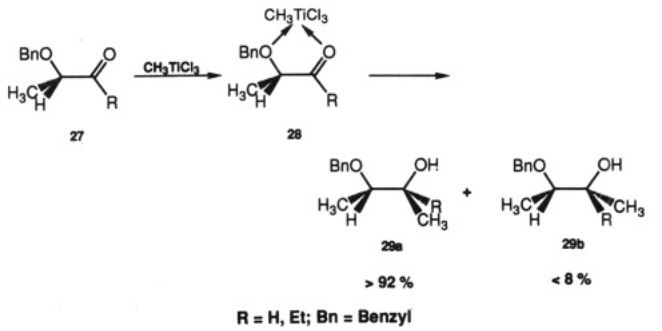

Scheme II

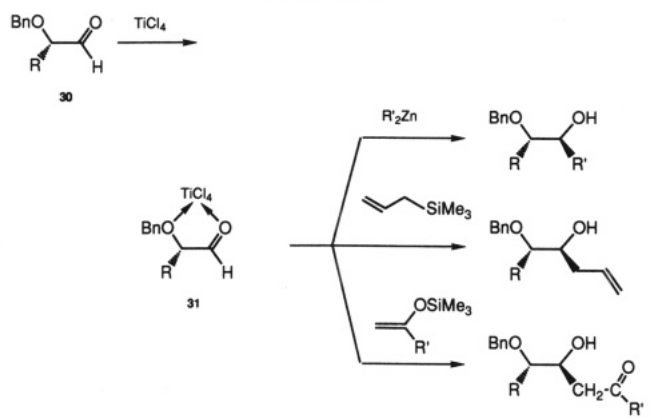

Table I. Basis Set Combinations Used in This Study

	basis Ti	splitting	basis Cl	basis H, C, N, O
I	TIVAL2-DZ	(51/31/41)	3-21G(d)	3-21G
II	HW3-DZ2P	(441/2111/41)	3-21G(d)	3-21G
III	HW3-TZ2P	(3311/2111/311)	6-31G(d)	6-31G(d)

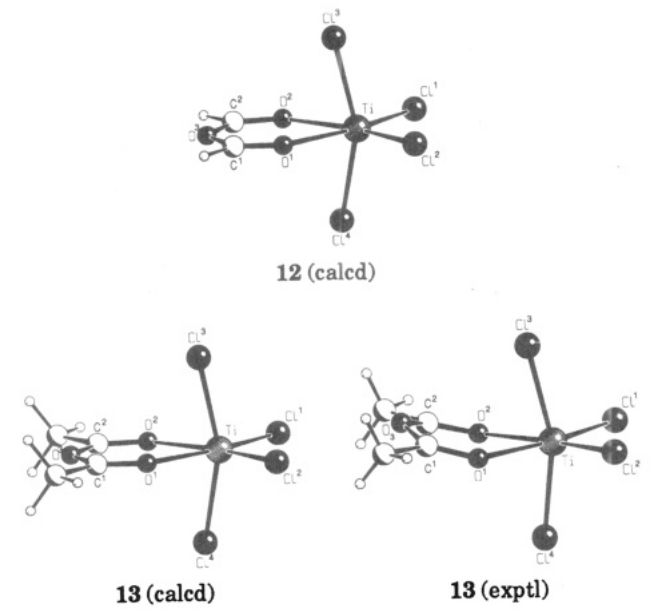

Figure 3. Theoretically predicted energy minimum structures of **12** and **13** and the experimental structure of **13**.

13 shows that the geometry has C_s symmetry;[5] the $TiCl_4$ unit is tilted toward one face of the five-membered subunit of the ring, which deviates from planarity with a torsion angle Ti–O(1)–C(1)–O(3) of 10.4°. The theoretical and experimental results agree that the axial chlorine ligands are bent toward the six-membered ring. The calculated small O(1)–Ti–O(2) angle of 74.1° is in good agreement

Table II. Theoretically Predicted and Experimentally Derived Bond Lengths (Å) and Bond Angles (deg) for 12–16

	12	**13**		
	calcd[a]	calcd[a]	calcd (fix)[b]	exptl[c]
Ti–Cl(1)	2.208 (2.204)	2.218 (2.214)	2.219	2.213
Ti–Cl(3)	2.305 (2.313)	2.317 (2.323)	2.341	2.318
Ti–Cl(4)	2.305 (2.313)	2.317 (2.323)	2.295	2.267
Ti–O(1)	2.212 (2.233)	2.158 (2.182)	2.154	2.162
C(1)–O(1)	1.204 (1.202)	1.211 (1.209)	1.212	1.213
C(1)–O(1)	1.367 (1.367)	1.375 (1.375)	1.376	1.362
Cl(1)–Ti–Cl(2)	102.1 (101.3)	101.6 (101.2)	101.6	100.0
Cl(3)–Ti–Cl(4)	157.4 (155.3)	159.5 (157.3)	160.1	161.1
O(1)–Ti–O(2)	73.5 (73.2)	74.1 (73.7)	75.2	76.1
C(1)–O(3)–C(2)	124.6 (124.9)	125.4 (125.7)	124.7	122.9
C(1)–O(1)–Ti	137.8 (137.7)	139.2 (139.2)	135.5	133.0
Ti–O(1)–C(1)–O(3)	0.0 (0.0)	0.0 (0.0)	9.5	10.4
E_{tot}(HF/III)	−2197.147 65	−2275.256 01	−2275.254 08	
E_{tot}(MP2/III)	−2198.801 73	−2277.165 16	−2277.164 37	
E_{rel}(HF/III)		0.0	1.2	
E_{rel}(MP2/III)		0.0	0.5	
symmetry	C_{2v}	C_{2v}	C_s	C_s

	14	**15**	**16**	
	calcd[a]	calcd	calcd	exptl[d]
Ti–Cl(1)	2.217 (2.212)	2.227	2.232	2.213
Ti–Cl(2)	2.217 (2.212)	2.227	2.232	2.229
Ti–Cl(3)	2.345 (2.355)	2.361	2.342	2.264
Ti–Cl(4)	2.293 (2.299)	2.299	2.325	2.300
Ti–O(1)	2.158 (2.174)	2.118	2.092	2.077
Ti–O(2)	2.158 (2.174)	2.118	2.092	2.086
C(1)–O(1)	1.219 (1.218)	1.226	1.228	1.229
C(2)–O(2)	1.219 (1.218)	1.226	1.228	1.231
Cl(1)–Ti–Cl(2)	101.4 (100.5)	101.2	101.0	99.9
Cl(3)–Ti–Cl(4)	158.8 (156.9)	160.9	161.7	166.1
O(1)–Ti–O(2)	75.1 (74.8)	75.5	74.6	78.1
C(1)–C(3)–C(2)	114.3 (114.2)	114.5	113.1	113.8
O(1)–C(1)–C(3)–C(2)	21.9 (22.9)	27.6	12.5	16.6
E_{tot}(HF/III)	−2161.302 91	−2239.406 53	−2317.467 30	
E_{tot}(MP2/III)	−2162.910 85	−2241.273 06	−2319.601 44	
symmetry	C_s	C_s	C_s	C_s

[a] The calculated values are obtained using basis set II; the values using basis set I are given in parentheses. E_{tot} values are given in hartrees and E_{rel} values in kcal/mol. [b] Angle O(3)–Ti–Cl(3) kept fixed at the experimental value. [c] Reference 5. [d] Reference 6.

with the experimental value of 76.1°. The experimentally derived axial Ti–Cl bond lengths differ by 0.05 Å (Table II). Except for the different symmetry of the molecule, the calculated and experimentally obtained geometries of **13** agree quite well. This is in agreement with the previous findings[2] that geometries of transition-metal complexes in high oxidation states are well-predicted at the HF level using basis set II. The bond lengths and angles have very similar values. In particular, the Ti–Cl bonds trans to the donor molecule are correctly predicted to be shorter than the cis Ti–Cl bonds.

We calculated **13** by freezing the angle O(3)–Ti–Cl(3) at the experimental value and optimizing the rest of the molecule. The predicted geometry is close to the experimental structure (Table II). In agreement with experiment, Ti–Cl(3) is calculated to be longer than Ti–Cl(4). The structure of **13** calculated with the experimental O(3)–Ti–Cl(3) angle is only 0.5 kcal/mol higher in energy than the energy minimum structure. It seems possible that the C_s geometry of **13** found by X-ray structure analysis[5] is caused by crystal-packing effects and that the isolated molecule has C_{2v} symmetry.

The comparison of **12** and **13** shows that the effect of the methyl groups is a decrease in the Ti–O bond length,

Table III. Calculated Energies (kcal/mol) for the Complex Formation of 12–16[a]

basis	ΔE_{12}	ΔE_{13}	ΔE_{14}	ΔE_{15}	ΔE_{16}
HF/III	−3.6	−14.0	−11.6	−17.0	−13.9
MP2/III	−9.3	−17.7	−16.9	−20.2	−16.5

[a] The energies have been calculated with the total energies given in ref 32.

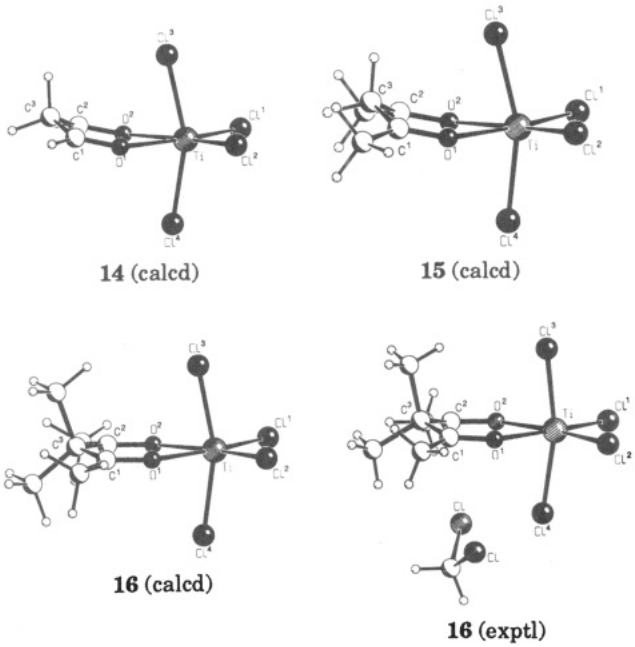

Figure 4. Theoretically predicted energy minimum structures of **14–16** and the experimental structure of **16**.

whereas the Ti–Cl bond distances increase. The shorter Ti–O bond indicates that the donor–acceptor interaction is stronger in **13** than in **12**. This is supported by the calculated energies of complex formation (Table III), which show that the complex formation energy for **13** (17.7 kcal/mol) is larger than for **12** (9.3 kcal/mol). The absolute values for the binding energies, which are calculated from the energy differences between the complexes and the donor and acceptor molecules in the corresponding energy minimum conformations,[32,33] may not be very accurate because of basis set limitation. However, we think that the relative values are correct because the error should cancel for the different structures.

$TiCl_4$ Complexes of 5–7 (Structures 14–16). The theoretically predicted energy minimum structures **14–16** and the experimental structure of **16** are shown in Figure 4. The calculated bond lengths and angles are summarized in Table II together with the experimental data for **16**.

The complexes **14–16** are theoretically predicted to have C_s symmetry (Figure 4); i.e., the six-membered ring is not planar. The torsion angle O(1)–C(1)–C(3)–C(2) is 21.9° for **14**, 27.6° for **15**, and 12.5° for **16**. This means that the substitution of an oxygen atom in **12** and **13** by a CH_2 group in **14** and **15** yields a change from C_{2v} to C_s symmetry. The calculated torsion angles indicate that the methyl groups at C(3) in **16** flatten the ring. The X-ray structure analysis of **16** shows a nearly C_s-symmetric molecule.[6] However, an additional CH_2Cl_2 molecule as a solvate at the bottom face of the molecule is found in the unit cell. The experiment also shows that the axial Ti–Cl bonds are different: Ti–Cl(3) is 0.036 Å shorter than Ti–Cl(4). The calculation gives the opposite trend: Ti–Cl(3) is 0.017 Å longer than Ti–Cl(4). The reverse order of the axial Ti–Cl bond distances may be an effect of the additional CH_2Cl_2 molecule. The steric interaction influences the tilt of the $TiCl_4$ moiety. The results for **13** discussed above show that this has a marked influence on the axial Ti–Cl bond lengths. Except for the axial Ti–Cl bond distances, the calculated and experimentally obtained geometries of **16** are very similar; the maximum differences are only 0.02 Å for the Ti–Cl and the Ti–O bonds.

Substitution of oxygen in **12** and **13** by a CH_2 group yields not only a change from C_{2v} to C_s symmetry for the equilibrium structures of **14** and **15**. The complex formation energies are also higher in the latter complexes (16.9 kcal/mol for **14**, 20.2 kcal/mol for **15**) than in the corresponding anhydride complexes (9.3 kcal/mol for **12**, 17.7 kcal/mol for **13**; Table III). The calculated data predict that the 1,3-dicarbonyl compounds **5** and **6** are stronger Lewis bases than the anhydrides **3** and **4**.[33]

Methyl substitution in **14–16** has a marked influence on the geometries: **15** has the largest torsion angle O(1)–C(1)–C(3)–C(2) and shows the largest difference between the Ti–Cl(3) and Ti–Cl(4) bond lengths (Figure 4, Table II). The effect of the methyl groups can also be seen in the metal–ligand bond lengths: the Ti–O bond distances become shorter, from 2.158 Å in **14** to 2.118 Å in **15** and to 2.092 Å in **16**, and the Ti–Cl(1) bond distances become longer. This shows that the donor–acceptor bond becomes stronger from the aldehyde **14** to the ketones **15** and **16**. The same trend is also predicted by the calculated energies of complex formation (Table III) for **14** (16.9 kcal/mol) and **15** (20.2 kcal/mol).[33] The smaller binding energy for **16** (16.5 kcal/mol) may be due to the steric repulsion in the sterically more crowded complex.

The calculated differences in the molecular geometries of **12** and **14** can be traced back to the different donor capabilities of the ligands. The Ti—O donor bond is 0.05 Å shorter in **14** than in **12**; the equatorial Ti—Cl and the C=O bonds are slightly longer. The optimized geometries also indicate that **5** is a better electron donor than **3**. The conjugation of the O(3) lone pair in **12** may be the reason for the planarity of the six-membered ring in **12** and **13**, whereas the six-membered ring in **14** and **15** is not planar.

$TiCl_4$ and CH_3TiCl_3 Complexes of Ethylene Glycol (17 and 18a,b). The theoretically predicted energy minimum structures of the hypothetical complexes **17** and **18a,b** are shown in Figure 5. The calculated bond lengths and angles are shown in Table IV.

Optimization of **17** gives a C_2-symmetric molecule which may be compared with the $TiCl_4$ adduct of 18-crown-6 studied by X-ray structure analysis.[12] The calculated complex is in reasonable agreement with experiment

(32) The calculated total energies for **1–11** (HF/III and MP2/III) are given in hartrees, and the respective symmetries are given in parentheses: **1** (T_d), −1895.655 35 (HF), −1896.536 07 (MP2); **2** (C_{3v}), −1475.739 01 (HF), −1476.601 11 (MP2); **3** (C_s), −301.486 64 (HF), −302.250 88 (MP2); **4** (C_2), −379.578 31 (HF), −380.600 92 (MP2); **5** (C_2), −265.629 06 (HF), −266.347 76 (MP2); **6** (C_2), −343.724 14 (HF), −344.704 83 (MP2); **7** (C_2), −421.789 75 (HF), −423.038 99 (MP2); **8** (C_1),[35] −228.919 77 (HF), −229.532.99 (MP2); **9** (C_1), −189.264 21 (HF), −189.847 67 (MP2); **10** (C_s), −227.758 88 (HF), −228.360 14 (MP2); **11a** (C_1), −266.799 01 (HF), −267.531 40 (MP2); **11b** (C_1), −305.845 17 (HF), −306.708 10 (MP2); **11c** (C_1), −305.822 53 (HF), 306.680 89 (MP2).

(33) (a) The energy minimum structure of **3** has a [cis,trans] conformation of the two carbonyl groups. Higher conformations are [cis, cis] ($E_{rel,MP2}$ = +2.4 kcal/mol) and [trans, trans] ($E_{rel,MP2}$ = +4.2 kcal/mol). (b) The energy minimum structure of **4** has a [cis, cis] conformation of the two carbonyl groups. The [cis, trans] conformation is 0.4 kcal/mol higher in energy (MP2/6-31G*). (c) The C_2-symmetric dicarbonyl structures of **5** and **6** were taken as reference structures.

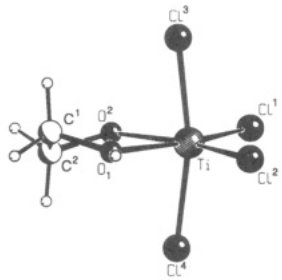

17

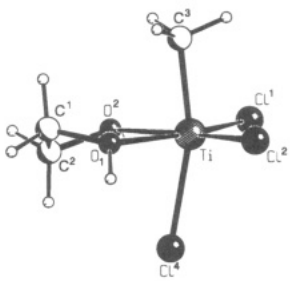

18a

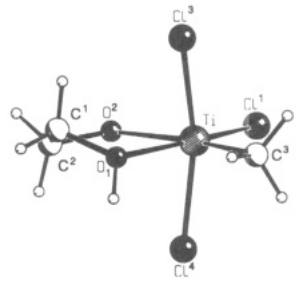

18b

Figure 5. Theoretically predicted energy minimum structures of **17** and **18a,b**.

(Table IV). The calculated Ti–O bond is 0.13 Å shorter and the equatorial Ti–Cl bonds are 0.04 Å longer in **17** than in **12**; the axial Ti—Cl bonds are 0.03 Å longer. The different Ti—O bond lengths in **17** and **12** indicate that a C—OH group is a better electron donor than a C=O group. The calculated complex formation energy of **17** (20.0 kcal/mol) is indeed clearly higher than for **12** (9.3 kcal/mol; Tables III, V, and VI).

Substitution of $TiCl_4$ in **17** by CH_3TiCl_3 yields **18a,b**, which show longer metal–ligand bond lengths. The complex formation energy, calculated at HF/III, is slightly higher for **17** than for **18a,b**, but the opposite order is predicted at MP2/III (Table V).

The Ti–Cl and Ti–O bonds are longer in **18a,b** than in **17**. This would indicate that **1** is a better Lewis acid than **2**.

The trans influence of the methyl groups at Ti increases the Ti–Cl(4) bond length in **18a** and the Ti–O(2) bond length in **18b** relative to the other isomer. The Ti–C(3) bond in **18a** is 0.03 Å longer than in **18b**, which shows the different trans influence of a chlorine ligand in **18a** and an OH group in **18b**. The five-membered rings in **18a,b** are distorted from the C_2-symmetric structure which is found for **17**. In **18a**, both OH groups are bent downward away from the methyl group; in **18b** only the O^1H^1 group is bent downward (Figure 5). There are two different axial Ti–Cl bond lengths in **18b**, although these bonds should be nearly equivalent. The reason for this may be the interaction of the methyl group at the metal with the O^1H^1 group, which makes the top and bottom sides of the molecule nonequivalent.

In agreement with the NMR studies of CH_3TiCl_3 adducts with glycol ether[14] the calculations predict that **18b** is lower in energy than **18a**. In order to gain insight as to why the isomer with the equatorial methyl group, **18b**, is more stable than **18a**, we calculated the donor and acceptor fragments in the frozen geometries of the complexes. The CH_3TiCl_3 conformations in the C_{3v} minimum[34] geometry **2** and in the complex geometries of **18a,b** are shown in Figure 6. Table VII shows the energies of distortion for the donor and acceptor fragments of **17** and **18a,b**. The results are very interesting. Complex **18b** is energetically favored over **18a** because the distortion of CH_3TiCl_3 from the equilibrium geometry is much lower in **18b** (31.0 kcal/mol) than in **18a** (41.1 kcal/mol). The binding energy of the distorted fragments CH_3TiCl_3 and ethylene glycol is higher in **18a** (76.0 kcal/mol) than in **18b** (68.0 kcal/mol). Thus, a trans chlorine atom actually *increases* the Lewis acidity of a transition-metal complex relative to a methyl group. In agreement with this, the calculated Ti–O(2) distance is shorter in **18a** (2.123 Å) than in **18b** (2.189 Å; Table IV). Isomer **18b** becomes more stable than **18a** only because of the significantly lower distortion energy of the CH_3TiCl_3 fragment (Table VII).

$TiCl_4$ and CH_3TiCl_3 Complexes of Ethylenediamine (19 and 20a,b). The theoretically predicted energy minimum structures **19** and **20a,b** are shown in Figure 7. The calculated bond lengths and angles are summarized in Table IV.

The results for the ethylenediamine complexes **19** and **20** are very similar to the ethylene glycol complexes **17** and **18**. Optimization of **19** yields a structure with C_2 symmetry. Because **9** is a better donor than **8**, the calculated binding energies are significantly higher for **19** and **20** than for **17** and **18** (Tables V and VI). The isomer **20b** with the methyl group in an equatorial position is predicted to be more stable than **20a**, which is in agreement with experimental evidence from NMR studies[14] and the calculated results for **18a,b**; the calculated energy difference between **20a** and **20b** is 1.3 kcal/mol. The complex formation energy is slightly higher for **19** than for **20a,b** at both HF/III and MP2/III (Table V).

$TiCl_4$ and CH_3TiCl_3 Complexes of 2-Hydroxyacetaldehyde (21 and 22a–c). The theoretically predicted energy minimum structures of **21** and **22a–c** are shown in Figure 8; Table IV lists the calculated bond lengths and angles.

The complex formation of **10** with $TiCl_4$ gives **21**, which has C_s symmetry. The donor strength of **10** should be intermediate between those of **5** and **8**. The calculated geometries and energies for **21** may be compared with those of **17** and **14**: both Ti–O bonds are longer in **21** than in **17** and shorter than in **14** (Tables II and IV). The calculated binding energy for **21** is 5.4 kcal/mol lower than for **17**, but it is also 2.3 kcal/mol higher than for **14** (Tables V and VI).

Three different isomeric structures are possible for the complex of **10** with CH_3TiCl_3. Structure **22a** has the methyl group in the axial position, while **22,c** have an equatorial methyl group. The calculated energies show that the lowest energy structure, **22b**, has the methyl group trans to the C–OH group. The complex formation energy is slightly lower for **21** than for **22b** at both HF/III and MP2/III (Table V).

(34) (a) Williamson, R. L.; Hall, M. B. *J. Am. Chem. Soc.* **1988**, *110*, 4428. (b) Williamson, R. L.; Hall, M. B. In *The Challenge of d and f Electrons-Theory and Computation*; Salahub, D. R., Zerner, M. C., Eds.; ACS Symposium Series 394; American Chemical Society: Washington, DC, 1989; p 17. (c) Krömer, R.; Thiel, W. *Chem. Phys. Lett.* **1992**, *189*, 105.

(35) (a) Cabral, B. J. C.; Albuquerque, L. M. P. C.; Fernandes, F. M. S. S. *Theor. Chim. Acta* **1991**, *78*, 271. (b) Murcko, M. A.; DiPaola, R. A. *J. Am. Chem. Soc.* **1992**, *114*, 10010.

Table IV. Theoretically Predicted and Experimentally Derived Bond Lengths (Å) and Bond Angles (deg) for 17–26

	17		18a	18b		17		18a	18b
	exptl[a]	calcd[b]	calcd[b]	calcd[b]		exptl[a]	calcd[b]	calcd[b]	calcd[b]
Ti–Cl(1)	2.229	2.242 (2.232)	2.270 (2.269)	2.264 (2.268)	Cl(1)–Ti–Cl(2)	100.6	107.8 (106.6)	107.9 (104.9)	
Ti–Cl(2)	2.221	2.242 (2.232)	2.262 (2.248)		Cl(1)–Ti–C(3)				102.9 (97.0)
Ti–Cl(3)	2.279	2.334 (2.342)		2.329 (2.336)	Cl(3)–Ti–Cl(4)	170.7	167.6 (165.3)		165.5 (160.5)
Ti–Cl(4)	2.285	2.334 (2.342)	2.476 (2.493)	2.383 (2.388)	C(3)–Ti–Cl(4)			164.0 (158.4)	
Ti–C(3)			2.084 (2.087)	2.056 (2.045)	O(1)–Ti–O(2)	74.6	72.4 (72.1)	72.7 (72.4)	71.2 (70.2)
Ti–O(1)	2.138	2.084 (2.102)	2.113 (2.143)	2.122 (2.130)	E_{tot}(HF/III)		−2124.602 99	−1704.680 22	−1704.685 65
Ti–O(2)	2.102	2.084 (2.102)	2.123 (2.146)	2.189 (2.242)	E_{tot}(MP2/III)		−2126.100 96	−1706.168 99	−1706.172 40
C(1)–O(1)		1.466 (1.466)	1.466 (1.465)	1.468 (1.469)	E_{rel}(HF/III)			3.4	0.0
C(2)–O(2)		1.466 (1.466)	1.466 (1.465)	1.458 (1.456)	E_{rel}(MP2/III)			2.1	0.0
					symmetry		C_2	C_1	C_1

	19	20a	20b		19	20a	20b
	calcd[b]	calcd[b]	calcd[b]		calcd[b]	calcd[b]	calcd[b]
Ti–Cl(1)	2.252 (2.242)	2.280 (2.274)	2.278 (2.262)	Cl(1)–Ti–Cl(2)	105.2 (104.7)	106.5 (106.4)	
Ti–Cl(2)	2.252 (2.242)	2.280 (2.272)		Cl(1)–Ti–C(3)			104.5 (101.1)
Ti–Cl(3)	2.341 (2.348)		2.362 (2.371)	Cl(3)–Ti–Cl(4)	163.1 (160.8)		165.9 (163.2)
Ti–Cl(4)	2.341 (2.348)	2.439 (2.452)	2.363 (2.370)	C(3)–Ti–Cl(4)		163.5 (160.8)	
Ti–C(3)		2.112 (2.112)	2.074 (2.066)	N(1)–Ti–N(2)	77.4 (76.7)	77.0 (76.4)	75.8 (75.2)
Ti–N(1)	2.196 (2.217)	2.209 (2.229)	2.221 (2.252)	E_{tot}(HF/III)	−2084.993 78	−1665.060 81	−1665.066 77
Ti–N(2)	2.196 (2.217)	2.213 (2.235)	2.265 (2.284)	E_{tot}(MP2/III)	−2086.471 00	−1666.530 35	−1666.532 50
C(1)–N(1)	1.504 (1.505)	1.500 (1.500)	1.502 (1.502)	E_{rel}(HF/III)		3.7	0.0
C(2)–N(2)	1.504 (1.505)	1.502 (1.503)	1.497 (1.497)	E_{rel}(MP2/III)		1.3	0.0
				symmetry	C_2	C_1	C_1

	21	22a	22b	22c		21	22a	22b	22c
	calcd[b]	calcd[b]	calcd[b]	calcd[b]		calcd[b]	calcd[b]	calcd[b]	calcd[b]
Ti–Cl(1)	2.209 (2.202)	2.240 (2.235)		2.246 (2.231)	Cl(1)–Ti–Cl(2)	104.7 (102.4)	106.2 (103.8)		
Ti–Cl(2)	2.243 (2.243)	2.273 (2.278)	2.262 (2.275)		Cl(1)–Ti–C(3)				99.6 (95.5)
Ti–Cl(3)	2.319 (2.324)		2.339 (2.340)	2.354 (2.368)	C(3)–Ti–Cl(2)			103.5 (96.5)	
Ti–Cl(4)	2.319 (2.324)	2.437 (2.438)	2.339 (2.340)	2.330 (2.343)	Cl(3)–Ti–Cl(4)	162.6 (159.9)		164.1 (158.9)	164.6 (159.5)
Ti–C(3)		2.084 (2.091)	2.044 (2.037)	2.067 (2.054)	C(3)–Ti–Cl(4)		159.9 (155.7)		
Ti–O(1)	2.153 (2.178)	2.186 (2.206)	2.236 (2.296)	2.190 (2.247)	O(1)–Ti–O(2)	69.9 (69.5)	69.3 (68.8)	68.6 (67.6)	68.8 (68.2)
Ti–O(2)	2.130 (2.146)	2.152 (2.171)	2.163 (2.160)	2.188 (2.257)	E_{tot}(HF/III)	−2123.432 09	−1703.509 40	−1703.516 55	−1703.512 90
C(1)–O(1)	1.443 (1.443)	1.447 (1.447)	1.439 (1.437)	1.445 (1.450)	E_{tot}(MP2/III)	−2124.919 55	−1704.986 26	−1704.988 11	−1704.987 24
C(2)–O(2)	1.220 (1.218)	1.220 (1.218)	1.219 (1.218)	1.217 (1.217)	E_{rel}(HF/III)		4.5	0.0	2.3
					E_{rel}(MP2/III)		1.2	0.0	0.6
					symmetry	C_s	C_1	C_s	C_1

	23	24a	24b		23	24a	24b
	calcd[b]	calcd[b]	calcd[b]		calcd[b]	calcd[b]	calcd[b]
Ti–Cl(1)	2.212 (2.203)	2.242 (2.236)	2.244 (2.239)	Cl(1)–Ti–Cl(2)	104.8 (102.4)	106.2 (103.9)	105.7 (103.1)
Ti–Cl(2)	2.245 (2.245)	2.273 (2.279)	2.274 (2.281)	Cl(3)–Ti–Cl(4)	163.4 (160.6)		
Ti–Cl(3)	2.326 (2.330)		2.427 (2.425)	C(3)–Ti–Cl(4)		160.4 (156.2)	
Ti–Cl(4)	2.318 (2.325)	2.438 (2.440)		Cl(3)–Ti–C(3)			161.0 (156.3)
Ti–C(3)		2.085 (2.091)	2.089 (2.095)	O(1)–Ti–O(2)	69.9 (69.5)	69.3 (68.7)	69.3 (68.7)
Ti–O(1)	2.146 (2.169)	2.178 (2.200)	2.178 (2.195)	E_{tot}(HF/III)	−2162.473 95	−1742.550 77	−1742.549 01
Ti–O(2)	2.125 (2.138)	2.147 (2.166)	2.142 (2.165)	E_{tot}(MP2/III)	−2164.093 07	−1744.159 15	−1744.158 36
C(1)–O(1)	1.452 (1.452)	1.455 (1.455)	1.453 (1.453)	E_{rel}(HF/III)		4.6	5.7
C(2)–O(2)	1.221 (1.219)	1.221 (1.219)	1.221 (1.219)	E_{rel}(MP2/III)		1.6	2.1
				symmetry	C_1	C_1	C_1

	24c	24d		24c	24d
	calcd[b]	calcd[b]		calcd[b]	calcd[b]
Ti–Cl(1)		2.250 (2.234)	Cl(1)–Ti–C(3)		99.2 (95.6)
Ti–Cl(2)	2.264 (2.275)		C(3)–Ti–Cl(2)	103.8 (96.6)	
Ti–Cl(3)	2.348 (2.355)	2.361 (2.373)	Cl(3)–Ti–Cl(4)	164.7 (159.7)	165.7 (160.1)
Ti–Cl(4)	2.336 (2.334)	2.331 (2.342)	O(1)–Ti–O(2)	68.5 (67.7)	68.8 (68.3)
Ti–C(3)	2.046 (2.038)	2.070 (2.056)	E_{tot}(HF/III)	−1742.558 13	−1742.553 98
Ti–O(1)	2.227 (2.291)	2.180 (2.237)	E_{tot}(MP2/III)	−1744.161 63	−1744.160 28
Ti–O(2)	2.160 (2.152)	2.175 (2.242)	E_{rel}(HF/III)	0.0	2.6
C(1)–O(1)	1.447 (1.444)	1.453 (1.456)	E_{rel}(MP2/III)	0.0	0.9
C(2)–O(2)	1.220 (1.219)	1.218 (1.217)	symmetry	C_s	C_1

	25a	25b	26a	26b		25a	25b	26a	26b
	calcd[c]	calcd[c]	calcd[c]	calcd[c]		calcd[c]	calcd[c]	calcd[c]	calcd[c]
Ti–Cl(1)		2.256		2.247	Cl(1)–Ti–C(3)		101.2		99.6
Ti–Cl(2)	2.271		2.270		C(3)–Ti–Cl(2)	103.5		100.7	
Ti–Cl(3)	2.357	2.370	2.349	2.350	Cl(3)–Ti–Cl(4)	165.8	167.3	165.6	166.1
Ti–Cl(4)	2.338	2.337	2.341	2.340	O(1)–Ti–O(2)	68.6	68.8	69.6	69.6
Ti–C(3)	2.048	2.074	2.047	2.065	E_{tot}(HF/III)	−1781.608 90	−1781.604 83	−1781.585 19	−1781.576 29
Ti–O(1)	2.225	2.167	2.230	2.221	E_{tot}(MP2/III)	−1783.342 44	−1783.341 16	−1783.319 09	−1783.313 62
Ti–O(2)	2.116	2.132	2.163	2.184	E_{rel}(HF/III)	0.0	2.5	0.0	5.6
C(1)–O(1)	1.447	1.454	1.442	1.453	E_{rel}(MP2/III)	0.0	0.8	0.0	3.5
C(2)–O(2)	1.227	1.225	1.220	1.219	symmetry	C_1	C_1	C_1	C_1
O(1)–C(5)			1.469	1.470					
C(1)–C(5)	1.494	1.493							

[a] Experiment $TiCl_4$ adduct of 18-crown-6.[12] [b] The calculated values are obtained using basis set II; the values using basis set I are given in parentheses. E_{tot} values are given in hartrees and E_{rel} values in kcal/mol. [c] The calculated values are obtained using basis set II.

Table V. Calculated Energies (kcal/mol) for the Complex Formation of 17–24

basis	ΔE_{17}	ΔE_{18a}	ΔE_{18b}	ΔE_{19}	ΔE_{20a}	ΔE_{20b}
HF/III	−17.5	−13.4	−16.7	−46.5	−36.1	−39.8
MP2/III	−20.0	−21.9	−24.0	−54.7	−51.2	−52.5

basis	ΔE_{21}	ΔE_{22a}	ΔE_{22b}	ΔE_{22c}
HF/III	−11.2	−7.2	−11.7	−9.4
MP2/III	−14.6	−15.7	−16.9	−16.3

basis	ΔE_{23}	ΔE_{24a}	ΔE_{24b}	ΔE_{24c}	ΔE_{24d}
HF/III	−12.3	−8.0	−6.9	−12.6	−10.0
MP2/III	−16.1	−16.7	−16.2	−18.3	−17.4

Table VI. Calculated Energies (kcal/mol) for Ligand-Exchange Reactions of 12–23

reacn	ΔE(HF/III)	ΔE(MP2/III)
4 + 12 → 3 + 13	−10.4	−8.4
5 + 12 → 3 + 14	−8.0	−7.6
6 + 14 → 5 + 15	−5.4	−3.3
7 + 15 → 6 + 16	+3.1	+3.7
8 + 12 → 3 + 17	−13.9	−10.7
2 + 17 → 1 + 18a	+4.1	−1.9
2 + 17 → 1 + 18b	+0.8	−4.0
9 + 17 → 8 + 19	−29.0	−34.7
2 + 19 → 1 + 20a	+10.4	+3.5
2 + 19 → 1 + 20b	+6.7	+1.2
10 + 12 → 3 + 21	−7.6	−5.3
10 + 14 → 5 + 21	+0.4	+2.3
10 + 17 → 8 + 21	+6.3	+5.4
11 + 21 → 10 + 23	−1.1	−1.5

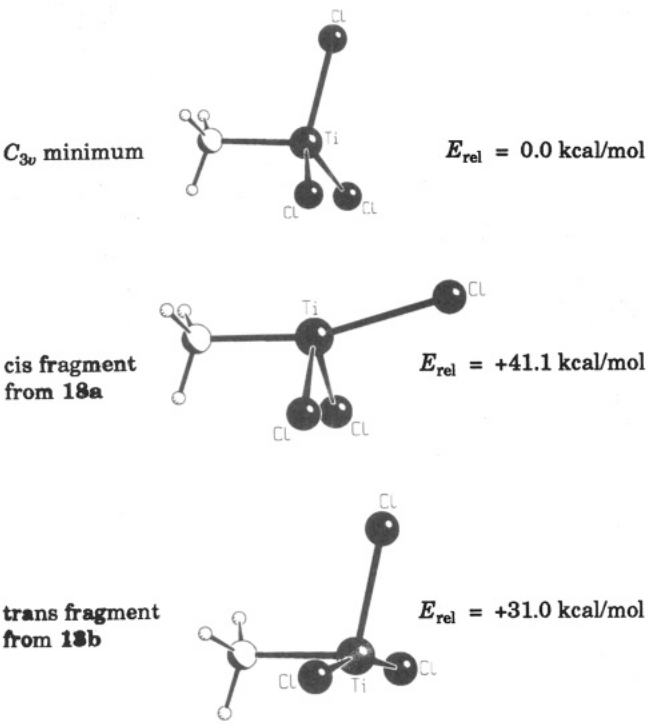

Figure 6. Conformations of CH_3TiCl_3 in the C_{3v} minimum geometry and in the geometries of the complexes **18a,b**.

In order to explain the energy difference between the two isomers **22b,c** with equatorial methyl groups, we calculated the donor and acceptor fragments in the frozen geometries of the complexes. Table VIII shows the energies of distortion for the donor and acceptor fragments of **21** and **22a–c**.

The breakdown of the energy contributions indicates clearly that structure **22a** has an energetically stronger distortion of the fragments from the equilibrium geometry (35.3 kcal/mol) than the isomers **22b** (27.7 kcal/mol) and **22c** (28.5 kcal/mol). This cannot be compensated by the stabilization energy of the fragments (Table VIII). Thus, although the attractive interaction energy of the fragments is stronger in **22a** (60.8 kcal/mol) than in **22b** (53.8 kcal/mol) and **22c** (54.2 kcal/mol), the net stabilization energy is larger for **22b**. In agreement with the higher binding energy between the fragments the Ti–O(1) and Ti–O(2) bonds in **22a** are shorter than in **22b** and **22c**. The higher stability of **22b** and **22c** over **22a** is caused by the more favorable geometry of the acceptor fragment (CH_3TiCl_3) rather than stronger donor–acceptor interactions. **22b** is favored over **22c**, but the energy differences are not very large (Table VIII).

Table VII. Energies (kcal/mol) of Distortion for the Fragments of 17 and 18a,b and Complex Formation Energies ΔE with and without Distortion

	distortion		ΔE	
structure and basis set	glycol	$TiCl_4$ and CH_3TiCl_3	rel to energy minima	rel to distorted fragments
17				
HF/III	+14.2	+39.9	−17.5	−71.6
MP2/III	+14.0	+37.2	−20.0	−71.3
18a				
HF/III	+13.4	+42.2	−13.4	−69.0
MP2/III	+13.0	+41.1	−21.9	−76.0
18b				
HF/III	+13.1	+27.2	−16.7	−57.0
MP2/III	+13.0	+31.0	−24.0	−68.0

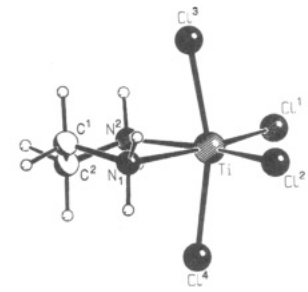

19

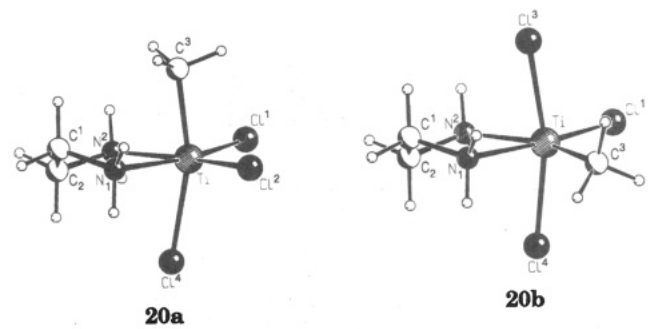

20a **20b**

Figure 7. Theoretically predicted energy minimum structures of **19** and **20a,b**.

$TiCl_4$ and CH_3TiCl_3 Complexes of (*S*)-2-Hydroxypropionaldehyde (23 and 24a–d). The theoretically predicted energy minimum structures of **23** and **24a–d** are displayed in Figure 9. The calculated bond lengths and angles are shown in Table IV.

The complex formation of **11** with $TiCl_4$ leads to **23**, with a nearly planar five-membered ring. The geometry of **23** is very similar to that of **21**; the calculated bond lengths and angles differ only slightly.

The adduct formation of **11** with CH_3TiCl_3 leads to four possible isomers. In **24a,b** the methyl group at Ti is axial; in the two other isomers it is either trans to C—OH (**24c**)

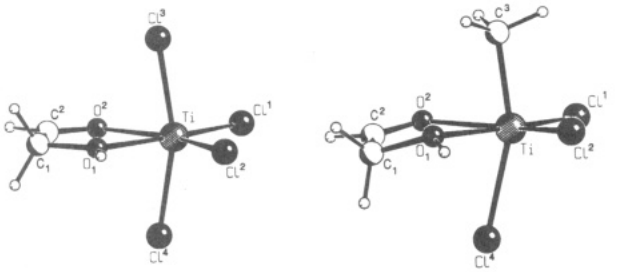

21 22a

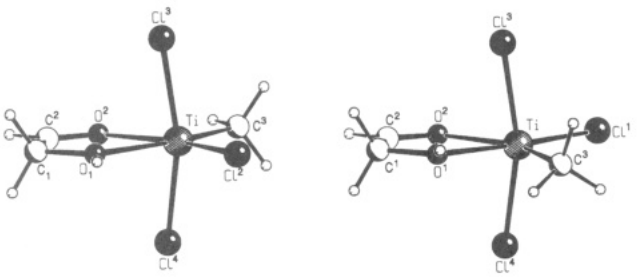

22b 22c

Figure 8. Theoretically predicted energy minimum structures of **21** and **22a–c**.

Table VIII. Energies (kcal/mol) of Distortion for the Fragments of 21 and 22a–c and Complex Formation Energies ΔE with and without Distortion

	distortion		ΔE	
structure and basis set	aldehyde	$TiCl_4$ and CH_3TiCl_3	rel to energy minima	rel to distorted fragments
21				
HF/III	+11.3	+33.7	−11.2	−56.3
MP2/III	+10.1	+31.2	−14.6	−55.9
22a				
HF/III	+11.3	+36.9	−7.2	−55.3
MP2/III	+9.9	+35.3	−15.7	−60.8
22b				
HF/III	+10.2	+24.4	−11.7	−46.3
MP2/III	+9.2	+27.7	−16.9	−53.8
22c				
HF/III	+10.4	+25.7	−9.4	−45.5
MP2/III	+9.4	+28.5	−16.3	−54.2

or trans to C=O (**24d**). As for **22a–c**, the calculated energies show that the most stable isomer, **24c**, has the methyl group trans to C—OH. The energies of **24a,b** are very similar; the difference between **24c** and **24d** is only 0.9 kcal/mol. The complex formation energy is slightly lower for **23** than for **24c** at both HF/III and MP2/III (Table V).

CH_3TiCl_3 Complexes of (*S*)-3-Hydroxybutan-2-one (25a,b) and (*S*)-2-Methoxypropionaldehyde (26a,b). In order to study the effect of an alkyl group upon the geometries and relative energies of the isomers **24c,d**, we calculated the methyl-substituted complexes **25a,b** and **26a,b**. The theoretically predicted energy minimum structures are displayed in Figure 10; the calculated bond lengths and angles are summarized in Table IV.

The optimized geometries differ not very much from those of the hydrogen-substituted molecules **24c,d**. The calculated Ti–O(1) bond length of **25a,b** is 0.03 Å shorter than in the aldehyde complexes. This shows the better donor capability of the ketone **11b** compared to the aldehyde **11a**. Table IX compares the complex formation energies of those complexes which have methyl groups at Ti trans to the chelating donor ligand.

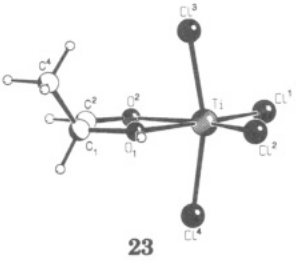

23

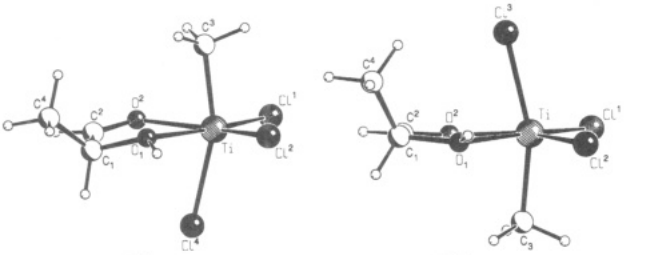

24a 24b

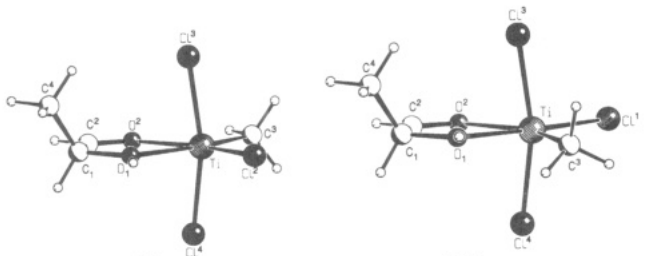

24c 24d

Figure 9. Theoretically predicted energy minimum structures of **23** and **24a–d**.

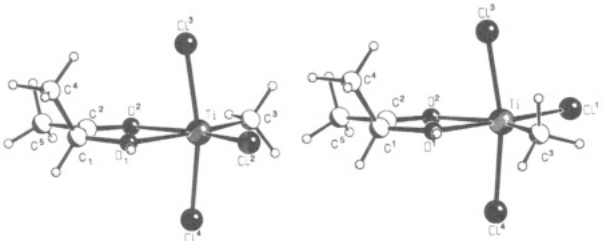

25a 25b

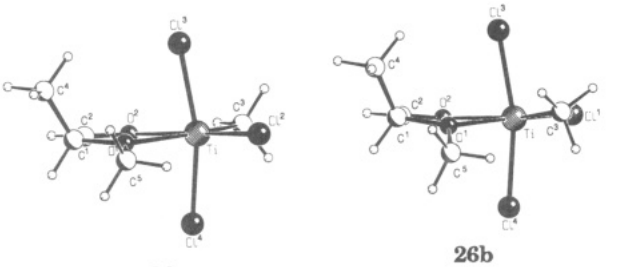

26a 26b

Figure 10. Theoretically predicted energy minimum structures of **25a,b** and **26a,b**.

The difference of complex formation energies between the isomers with equatorial methyl groups at Ti is about 0.6–0.9 kcal/mol for the aldehyde and ketone complexes **22b/22c**, **24c/24d**, and **25a/25b**. It changes to 3.5 kcal/mol for the ether complexes **26a/26b**. We believe that this is an effect of the molecular geometry of **26b** (see Figure 10): the ether group and the methyl group at Ti are in cis positions relative to each other, which results in a higher steric repulsion than in **26a**. From the calculations we conclude that the relative stability of complexes with

Table IX. Comparison of the Calculated Complex Formation Energies for All Structures with the Methyl Group at Ti Trans to the Chelating Ligand (kcal/mol)

structure 1[a]	structure 2[b]	ΔE_1	ΔE_2	$\Delta\Delta E$
22b	**22c**			
HF/III	HF/III	−11.7	−9.4	2.3
MP2/III	MP2/III	−16.9	−16.3	0.6
24c	**24d**			
HF/III	HF/III	−12.6	−10.0	2.6
MP2/III	MP2/III	−18.3	−17.4	0.9
25a	**25b**			
HF/III	HF/III	−15.5	−13.0	2.5
MP2/III	MP2/III	−20.8	−20.0	0.8
26a	**26b**			
HF/III	HF/III	−14.8	−9.2	5.6
MP2/III	MP2/III	−23.3	−19.8	3.5

[a] Structure 1 = methyl group at titanium trans to C=O. [b] Structure 2 = methyl group at Ti trans to OH/OCH_3.

equatorial methyl groups at Ti is not very different between the aldehyde complexes **24c/24d** and the ketone complexes **25a/25b**. Groups larger than methyl at O(1) may yield a higher stability of **26a** analogs.

Experimentally, the reaction of **27** (R = Et) with CH_3TiCl_3 under kinetic conditions leads to two isomers of **28** (Scheme I, R = Et).[19] One of the isomers reacts to form **29a** (R = Et) faster than the other isomer. On the basis of the present calculations and the experimental observations we suggest that the observed isomers of **28** are those in which the methyl group at titanium is trans to the carbonyl and ether functions, respectively.

Summary

The optimized geometries and relative stabilities for the chelate complexes of $TiCl_4$ and CH_3TiCl_3 **12–26** are in satisfactory agreement with experimental results. The calculated binding energies for the complex formation indicate that the Lewis acidity of $TiCl_4$ is comparable in magnitude to that of CH_3TiCl_3 and that the donor strength of the Lewis bases increases with $NH_2 \gg OH > O{=}C$.

The lowest energy isomer of CH_3TiCl_3 complexes has the methyl group in the equatorial position rather than in the axial position. The higher stability of the isomer with an equatorial methyl group is, however, not caused by the stronger donor–acceptor interactions with the chelate ligand, which are stronger in the isomer with the methyl group being axial. The latter isomer has a much higher deformation of the CH_3TiCl_3 fragment which yields a lower net stabilization. The energy differences between the isomers with equatorial methyl groups are small.

Acknowledgment. This study was supported by the Deutsche Forschungsgemeinschaft (SFB 260 and Leibniz program) and the Fonds der Chemischen Industrie. Additional support has been provided by the computer companies Convex and Silicon Graphics. V.J. thanks the Fonds der Chemischen Industrie for a predoctorate scholarship. We thank the HLRZ Jülich and the TH Darmstadt for additional computer time on the Cray Y-MP 832 and the Fujitsu S400/40 supercomputers.

OM9208228